

*Exceptional service in the national interest*



# Progress and Challenges in Computational Peridynamics

David Littlewood

Workshop on Nonlocal Models in Mathematics, Computation, Science, and Engineering  
28 October 2015



Center for Computing Research



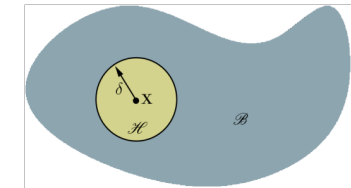
Sandia National Laboratories is a multi-program laboratory managed and operated by Sandia Corporation, a wholly owned subsidiary of Lockheed Martin Corporation, for the U.S. Department of Energy's National Nuclear Security Administration under contract DE-AC04-94AL85000. SAND2015-XXXX

# Peridynamic Theory of Solid Mechanics

Peridynamics is a mathematical theory that unifies the mechanics of continuous media, cracks, and discrete particles

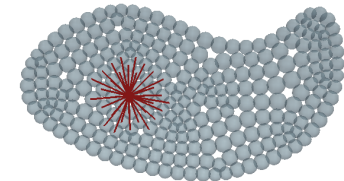
- Peridynamics is a nonlocal extension of continuum mechanics
- Remains valid in presence of discontinuities, including cracks
- Balance of linear momentum is based on an integral equation

$$\rho(\mathbf{x})\ddot{\mathbf{u}}(\mathbf{x}, t) = \underbrace{\int_{\mathcal{B}} \{\underline{\mathbf{T}}[\mathbf{x}, t] \langle \mathbf{x}' - \mathbf{x} \rangle - \underline{\mathbf{T}}'[\mathbf{x}', t] \langle \mathbf{x} - \mathbf{x}' \rangle\} dV_{\mathbf{x}'} + \mathbf{b}(\mathbf{x}, t)}_{\text{Divergence of stress replaced with integral of nonlocal forces.}}$$



- Peridynamic bonds connect any two material points that interact directly
- Peridynamic forces are determined by force states acting on bonds
- A peridynamic body may be discretized by a finite number of elements

$$\rho(\mathbf{x})\ddot{\mathbf{u}}_h(\mathbf{x}, t) = \sum_{i=0}^N \{\underline{\mathbf{T}}[\mathbf{x}, t] \langle \mathbf{x}'_i - \mathbf{x} \rangle - \underline{\mathbf{T}}'[\mathbf{x}'_i, t] \langle \mathbf{x} - \mathbf{x}'_i \rangle\} \Delta V_{\mathbf{x}'_i} + \mathbf{b}(\mathbf{x}, t)$$



S.A. Silling. Reformulation of elasticity theory for discontinuities and long-range forces. *Journal of the Mechanics and Physics of Solids*, 48:175-209, 2000.

S.A. Silling and E. Askari. A meshfree method based on the peridynamic model of solid mechanics. *Computers and Structures*, 83:1526-1535, 2005.

Silling, S.A. and Lehoucq, R. B. Peridynamic Theory of Solid Mechanics. *Advances in Applied Mechanics* 44:73-168, 2010.

# The *Peridigm* Computational Peridynamics Code

## WHAT IS PERIDIGM?

- Open-source software developed at Sandia National Laboratories
- C++ code based on Sandia's *Trilinos* project
- Platform for multi-physics peridynamic simulations
- Capabilities:
  - State-based constitutive models
  - Implicit and explicit time integration
  - Contact for transient dynamics
  - Large-scale parallel simulations
- Compatible with pre- and post-processing tools
  - Cubit mesh generation
  - Paraview visualization tools
  - SEACAS utilities
- Designed for extensibility



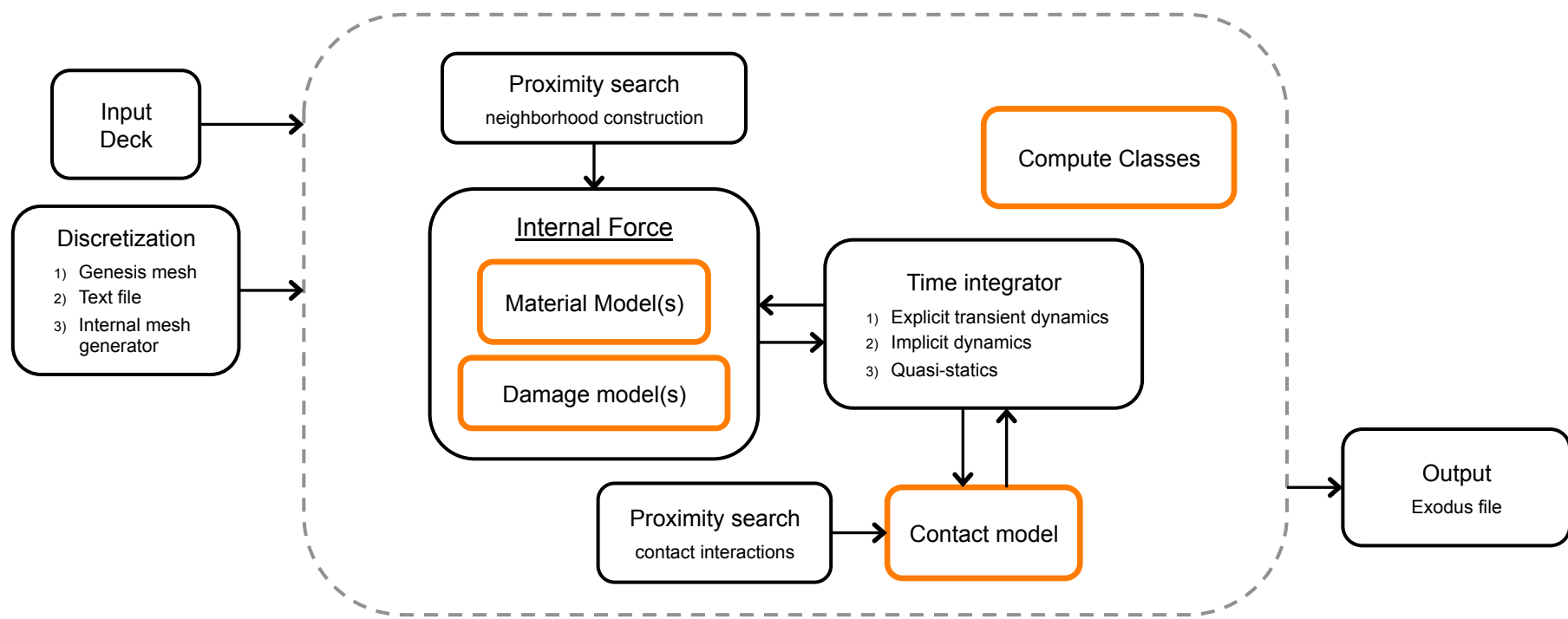
## Contributors

Michael Parks	John Foster, et al.
David Littlewood	Stewart Silling
John Mitchell	Alex Vasenkov
Dan Turner	

# Peridigm Code Architecture

## DESIGN GOALS:

- State-based peridynamics
- Explicit and Implicit time integration
- Proximity search neighborhood construction
- Contact
- Massively parallel
- Performance
- Extensibility



Orange denotes extensible components

# Ingredients for Computational Peridynamics

- Constitutive model
- Bond-failure law
- Contact model
- Discretization
- Time integration
  - Explicit
  - Implicit
- Pre- and post-processing
- Model coupling

# Constitutive Models for Peridynamics

## PERIDYNAMIC FORCE STATES MAP BONDS TO PAIRWISE FORCE DENSITIES

- Peridynamic constitutive laws can be grouped into two categories
  - *Bond-based*: bond forces depend only on a single pair of material points
  - *State-based*: bond forces depend on deformations of all neighboring material points

### Microelastic Material <sup>1</sup>

- Bond-based constitutive model
- Pairwise forces are a function of bond stretch

$$s = \frac{y - x}{x}$$

- Magnitude of pairwise force density given by

$$\underline{t} = \frac{18k}{\pi\delta^4} s$$

### Linear Peridynamic Solid <sup>2</sup>

- State-based constitutive model
- Deformation decomposed into deviatoric and dilatational components

$$\theta = \frac{3}{m} \int_{\mathcal{H}} (\underline{\omega} \underline{x}) \cdot \underline{e} dV \quad \underline{e}^d = \underline{e} - \frac{\theta \underline{x}}{3}$$

- Magnitude of pairwise force density given by

$$\underline{t} = \frac{3k\theta}{m} \underline{\omega} \underline{x} + \frac{15\mu}{m} \underline{\omega} \underline{e}^d$$

### Definitions

$\underline{x}$	bond vector
$x$	initial bond length
$y$	deformed bond length
$s$	bond stretch
$\underline{e}$	bond extension
$\underline{e}^d$	deviatoric bond extension
$\underline{\omega}$	influence function
$V$	volume
$\mathcal{H}$	neighborhood
$m$	weighted volume
$\theta$	dilatation
$\delta$	horizon
$k$	bulk modulus
$\mu$	shear modulus
$\underline{t}$	pairwise force density

1. S.A. Silling. Reformulation of elasticity theory for discontinuities and long-range forces. *Journal of the Mechanics and Physics of Solids*, 48:175-209, 2000.
2. S.A. Silling, M. Epton, O. Weckner, J. Xu, and E. Askari, Peridynamic states and constitutive modeling, *Journal of Elasticity*, 88, 2007.

# Classical Material Models Can Be Applied in Peridynamics



*CORRESPONDENCE APPROACH RESULTS IN A NON-ORDINARY STATE-BASED MATERIAL MODEL*<sup>1</sup>

- Approximate deformation gradient based on initial and current locations of material points in family

## Approximate Deformation Gradient

$$\bar{\mathbf{F}} = (\underline{\mathbf{Y}} * \underline{\mathbf{X}}) \mathbf{K}^{-1}$$

## Shape Tensor

$$\mathbf{K} = \underline{\mathbf{X}} * \underline{\mathbf{X}}$$

## Definitions

$\underline{\mathbf{X}}$	reference position
$\underline{\mathbf{Y}}$	vector state
$\mathbf{K}$	deformation vector state
$\bar{\mathbf{F}}$	shape tensor
$\underline{\mathbf{F}}$	approximate deformation gradient
$\xi$	bond
$\underline{\omega}$	influence function
$\sigma$	Piola stress

- Kinematic data passed to classical material model
- Classical material model computes stress
- Stress converted to pairwise force density

$$\underline{\mathbf{T}}(\xi) = \underline{\omega}(\xi) \sigma \mathbf{K}^{-1} \xi$$

- Suppression of zero-energy modes (optional)<sup>2</sup>

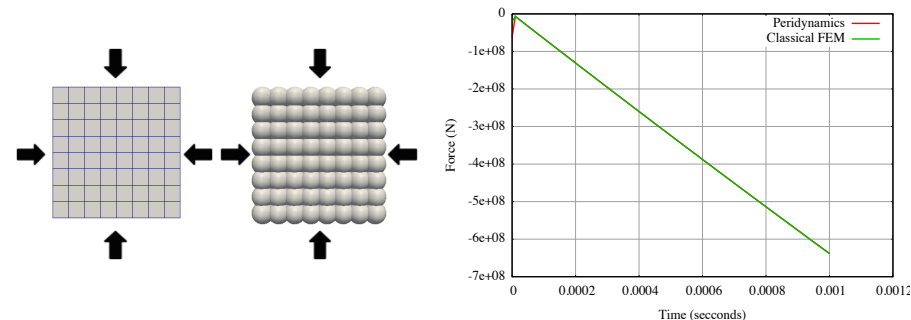
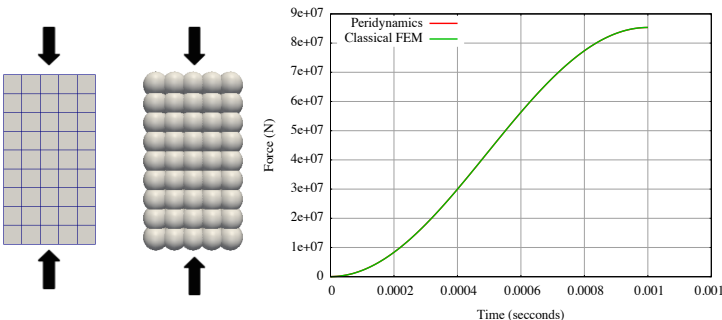
1. S.A. Silling, M. Epton, O. Weckner, J. Xu, and E. Askari, Peridynamic states and constitutive modeling, *Journal of Elasticity*, 88, 2007.

2. Littlewood, D. A Nonlocal Approach to Modeling Crack Nucleation in AA 7075-T651. Proceedings of the ASME 2011 International Mechanical Engineering Congress and Exposition, Denver, Colorado, 2011.

# Examples of Verification Problems

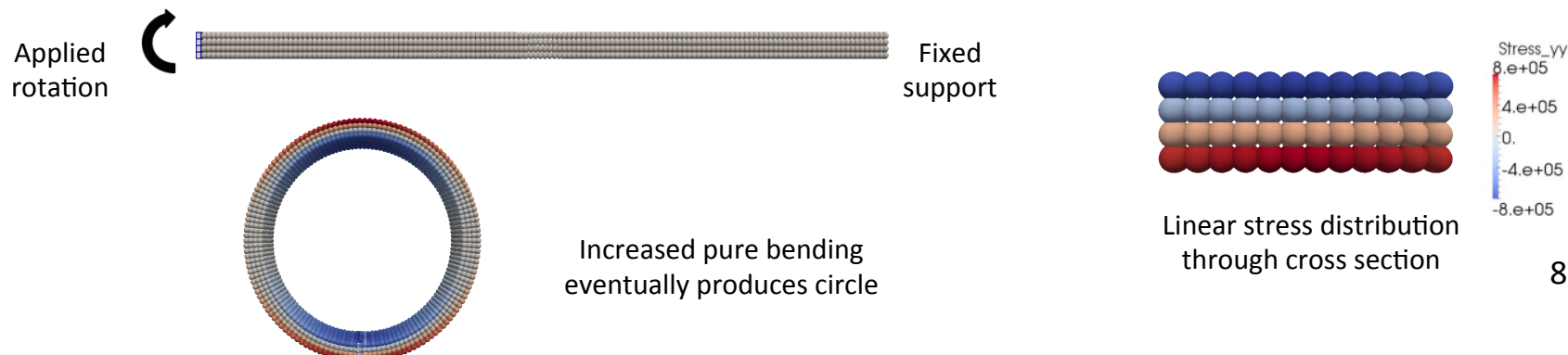
## Uniaxial and hydrostatic compression

- Tests constructed such that peridynamics and classical FEM should yield same result
- Simulation results verified for numerous material models



## Beam bending

- Test peridynamics with neo-Hookean material model against classical beam bending theory
- Simulation gives expected bending response and stress distribution



# Position-Aware Linear Solid Material Model

## ADDRESSES SURFACE EFFECT

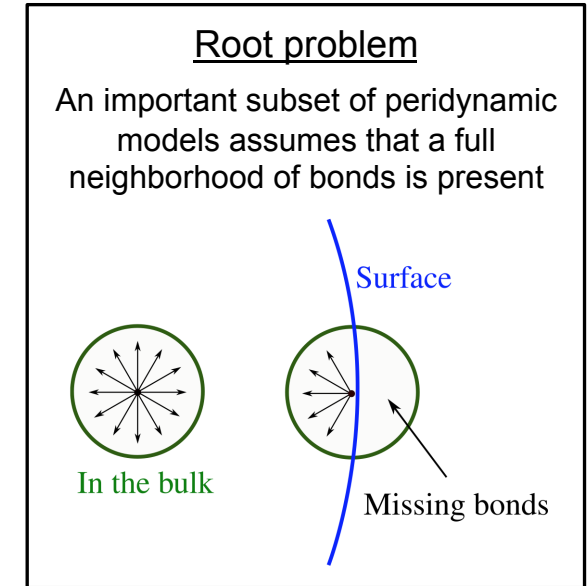
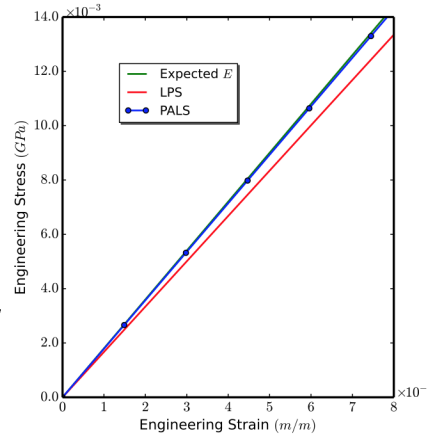
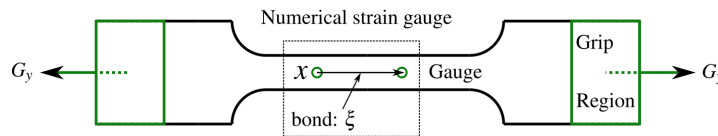
- Position-Aware Linear Solid (PALS) constitutive model takes proximity to free surfaces into account

$$W = \frac{1}{2}K\theta^2 + \mu(\underline{\sigma}\underline{\epsilon}) \bullet \underline{\epsilon}, \quad \theta = (\underline{\omega}|X|) \bullet \underline{\epsilon}$$

- Coefficients  $\sigma$  and  $\omega$  are determined for each point in the discretized model
- Calculation of  $\sigma$  and  $\omega$  ensures that the expected strain energy is recovered for a set of *matching deformations*

### Example calculation

PALS model accurately recovers elastic modulus in tensile test



# Ingredients for Computational Peridynamics

- Constitutive model
- Bond-failure law
- Contact model
- Discretization
- Time integration
  - Explicit
  - Implicit
- Pre- and post-processing
- Model coupling

# Material Failure Is Controlled by a Bond-Failure Law

## THE CRITICAL-STRETCH MODEL IS THE SIMPLEST BOND-FAILURE LAW

- A bonds fails irreversibly when its stretch exceeds a critical value

$$s_{\max} = \frac{y_{\max} - x}{x} \quad d = \begin{cases} 0 & \text{if } s_{\max} < s_0 \\ 1 & \text{if } s_{\max} \geq s_0 \end{cases}$$

- The critical stretch value is a function of the energy release rate

$$s_0 = \sqrt{\frac{5G_o}{9k\delta}}$$

## EXAMPLES OF OTHER BOND-FAILURE LAWS

- Modifications of critical stretch law for pervasive damage [Silling]
- Energy-based approach [Foster]
- Ductile failure models for peridynamics [Silling]

Silling, S.A. and Askari, E. A meshfree method based on the peridynamic model of solid mechanics. *Computers and Structures* 83:1526-1535, 2005.

SIERRA Solid Mechanics Team. Sierra/SolidMechanics 4.36 user's guide. SAND Report 2015-2199, Sandia National Laboratories, Albuquerque, NM and Livermore, CA.

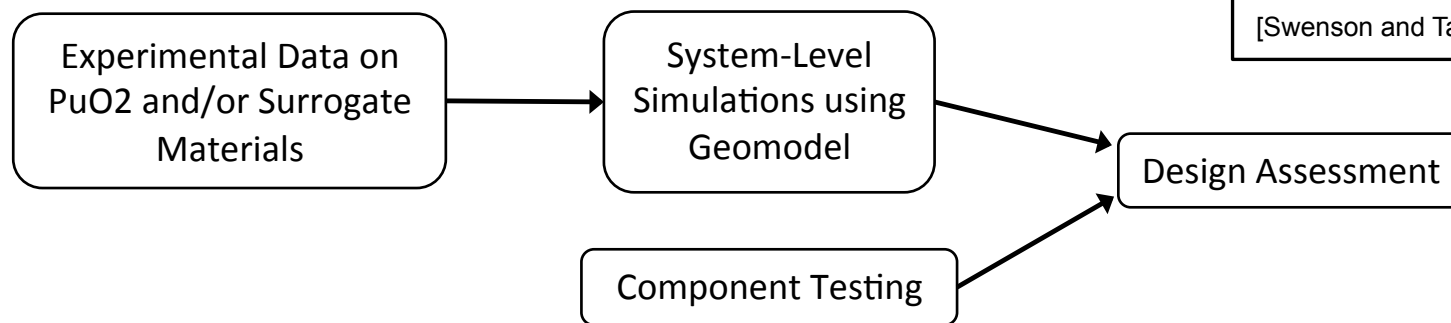
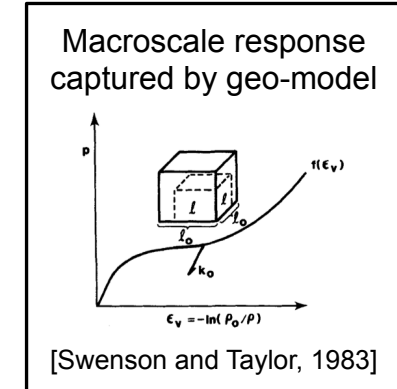
Foster, J.T., Silling, S.A., and Chen, W. An energy based failure criterion for use with peridynamic states. *Journal for Multiscale Computational Engineering* 9(6): 675-687, 2011.

Littlewood, D.J., Silling, S.A., Mitchell, J.A., Seleson, P.D., Bond, S.D., Parks, M.L., Turner, D.Z., Burnett, D.J., Ostien, J. and Gunzburger, M. Strong local-nonlocal coupling for integrated fracture modeling. SAND Report 2015-7998, Sandia National Laboratories, Albuquerque, NM and Livermore, CA.

# Example Simulation: Grain-Scale Modeling of Fuel Pellets

## DESIGN ASSESSMENT BASED ON EXPERIMENTS AND SIMULATIONS

- Performing experiments on  $\text{PuO}_2$  is difficult and expensive
- Key role for computational simulation
- Macroscale material response captured by continuum model



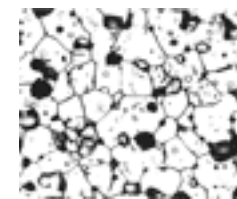
## MECHANICAL PROPERTIES DICTATED BY FABRICATION, STORAGE, AND SERVICE CONDITIONS



Pressed  
 $\text{PuO}_2$  pellet



Sintered pellet  
at 1400 °C

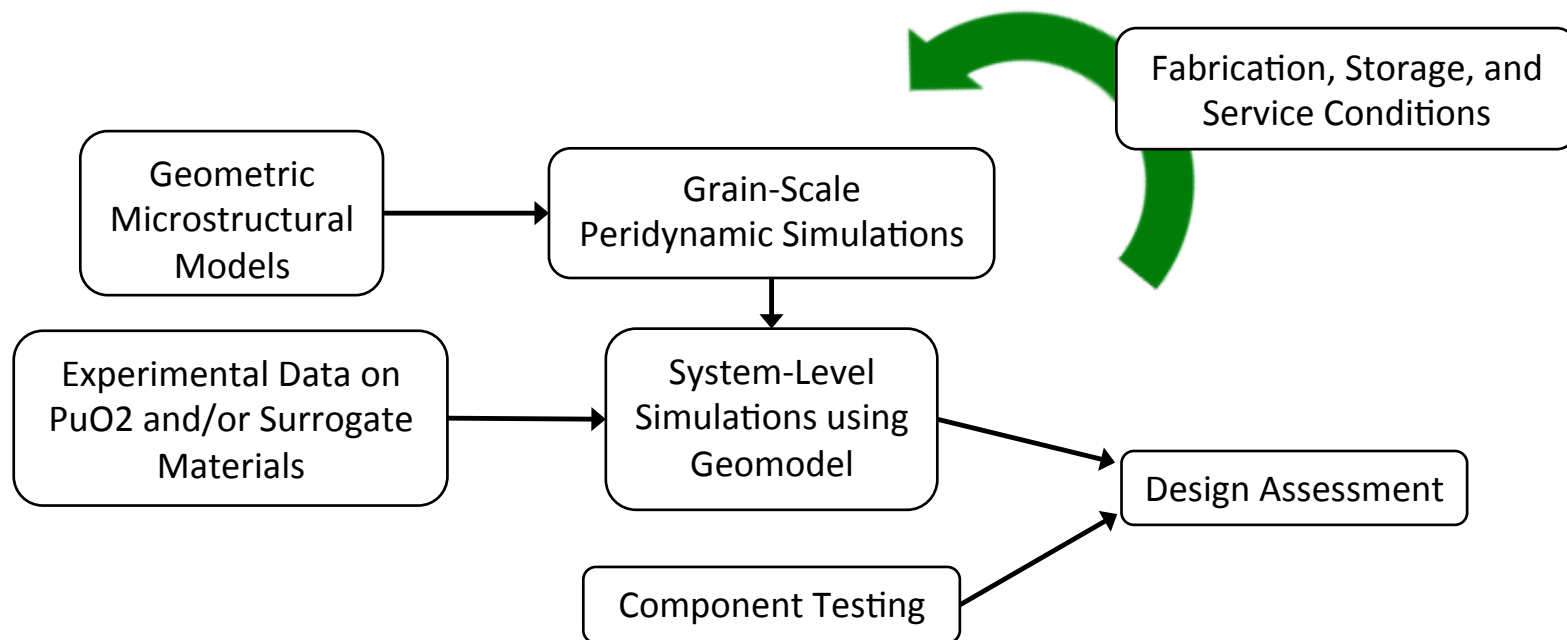


Sintered pellet  
at 1700 °C

# Example Simulation: Grain-Scale Modeling of Fuel Pellets

## CAN WE MOVE BEYOND DESIGN ASSESSMENT?

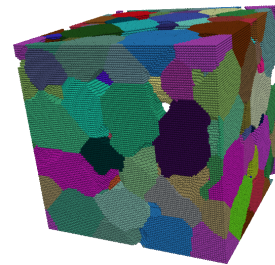
- The grain structure is dictated by fabrication, storage, and service conditions
- Mechanical response is largely determined by grain-scale mechanisms
- There is potential to alter fabrication, storage, and service conditions for improved mechanical performance based on simulation results



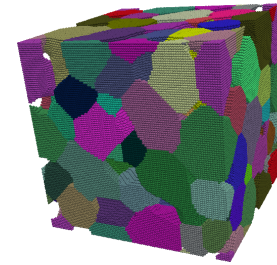
# Example Simulation: Grain-Scale Modeling of PuO<sub>2</sub>

## REPRESENTATIONAL VOLUMES CAPTURE CRITICAL GRAIN-SCALE FEATURES

- Microstructure evolution model captures effects of fabrication conditions [Tikare, et al.]
- Key features:
  - Grain size, shape
  - Void fraction



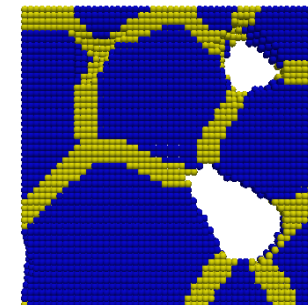
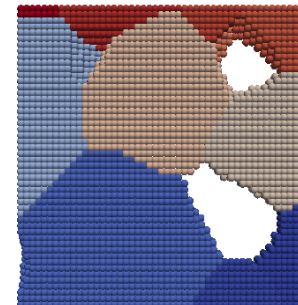
15% void volume



20% void volume

## APPLY PERIDYNAMIC MODEL AT GRAIN-SCALE

- Individual grain response modeled as elastic
- Modified critical-stretch bond failure
- Contact algorithm controls material interactions after bonds are broken



**Bond-failure law applied only to bonds across grain boundaries**

Tikare, V., Braginsky, M., Bouvard, D., and Vagnon, A. Numerical simulation of microstructural evolution during sintering at the mesoscale in a 3D powder compact, *Computational Materials Science* 48:317-325, 2010.

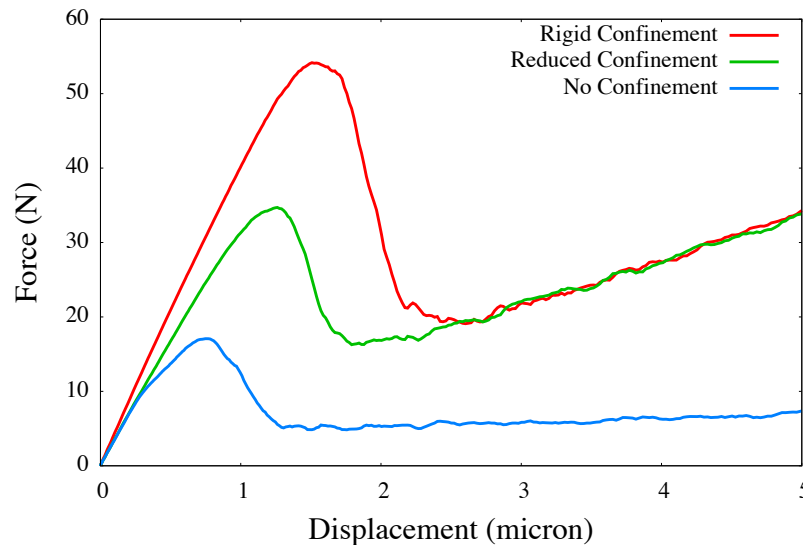
D. Littlewood, V. Tikare, and J. Bignell. Informing Macroscale Constitutive Laws through Modeling of Grain-Scale Mechanisms in Plutonium Oxide. Workshop on Nonlocal Damage and Failure: Peridynamics and Other Nonlocal Models, San Antonio, Texas, March 11-12 2013.

# Example Simulation: Grain-Scale Modeling of PuO<sub>2</sub>

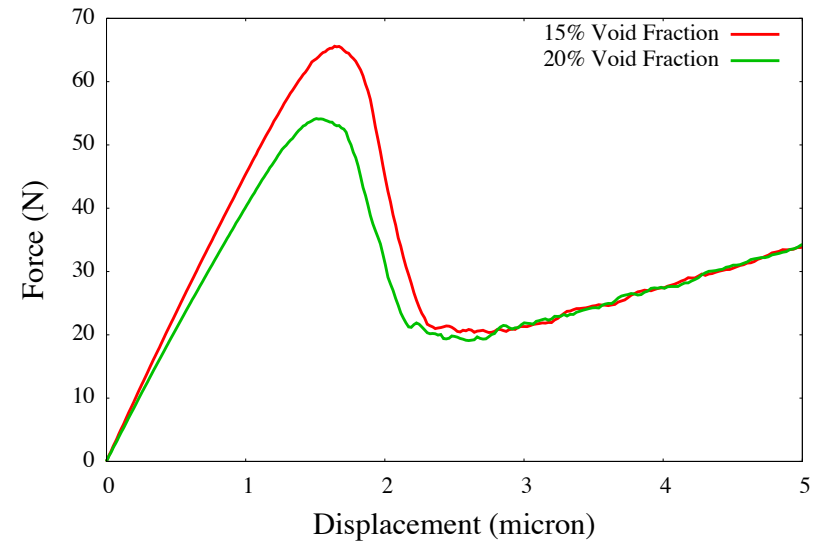


*REPRESENTATIONAL VOLUMES CAPTURE CRITICAL GRAIN-SCALE FEATURES*

Effect of confinement



Effect of void fraction



# Ingredients for Computational Peridynamics

- Constitutive model
- Bond-failure law
- **Contact model**
- Discretization
- Time integration
  - Explicit
  - Implicit
- Pre- and post-processing
- Model coupling

# Short-Range Force Contact Model

*SHORT-RANGE FORCE MODEL MAY INCLUDE STATIC AND DAMPING TERMS*

$$\mathbf{f}_{\text{static}} = A C_{ij} \left( \frac{d - |\mathbf{y}_j - \mathbf{y}_i|}{d} \right) \Delta V_i \Delta V_j \mathbf{M}_{ij}$$

$$C_{ij} = \frac{18k}{\pi \delta^4} \quad \mathbf{M}_{ij} = \frac{\mathbf{y}_j - \mathbf{y}_i}{|\mathbf{y}_j - \mathbf{y}_i|}$$

Force is zero unless distance  
between nodes is less than  $d$        $d_{ij} = \min \{ \beta |\mathbf{x}_j - \mathbf{x}_i|, \alpha(r_i + r_j) \}$

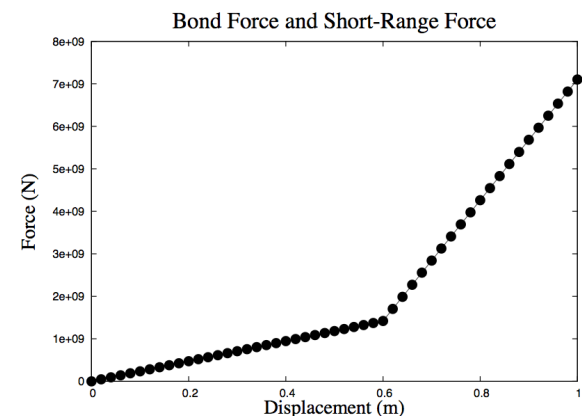
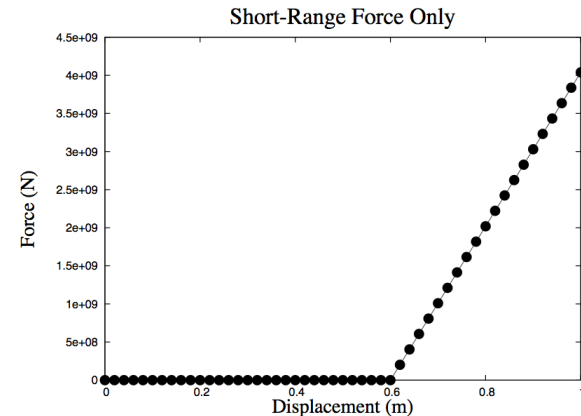
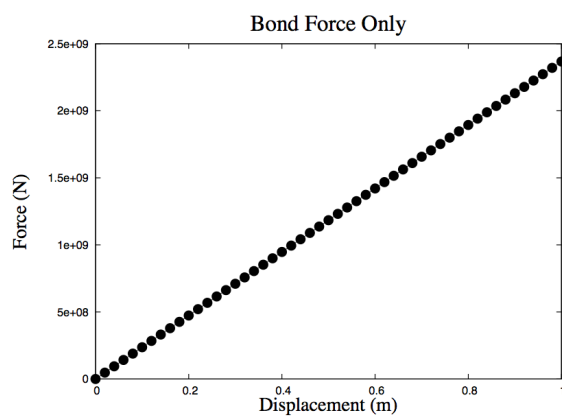
$$\mathbf{f}_{\text{damping}} = \epsilon \gamma_c v_{ij} \mathbf{M}_{ij}$$

Critical damping constant       $\gamma_c = 2\sqrt{A C_{ij} \Delta V_i \Delta V_j \bar{m}}$

Relative separation velocity       $v_{ij} = (\mathbf{v}_j - \mathbf{v}_i) \cdot \mathbf{M}_{ij}$

# Short-Range Force Contact Model

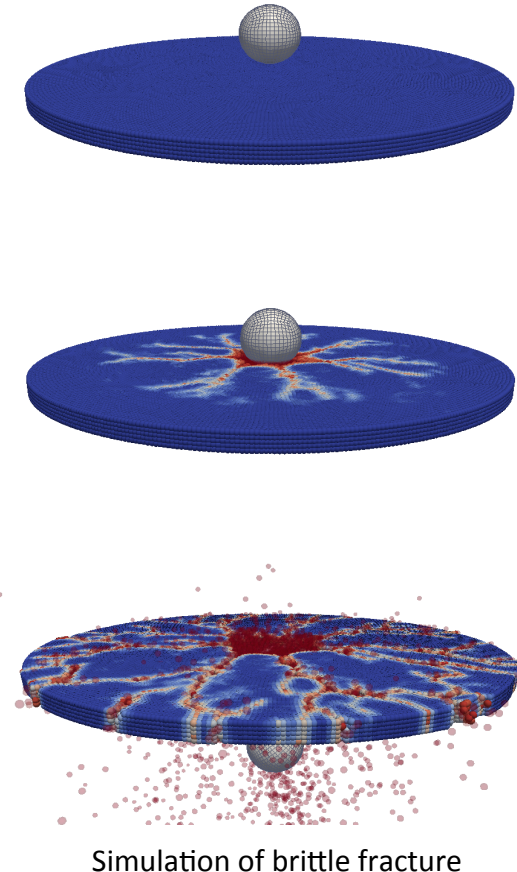
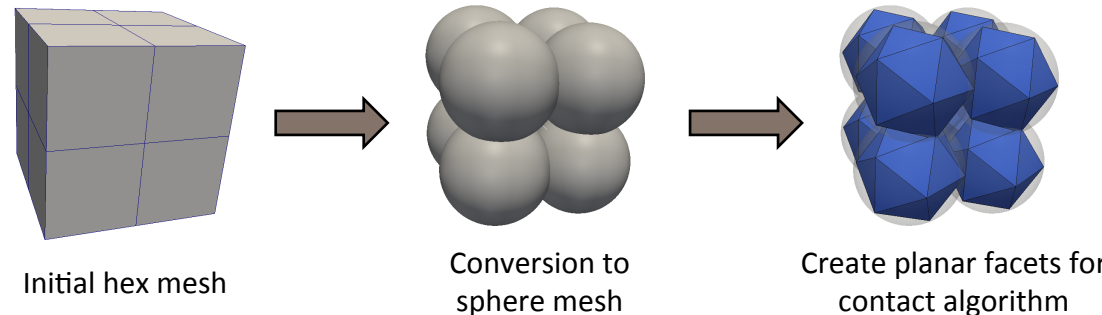
## ILLUSTRATION OF SHORT-RANGE FORCE AND STANDARD BOND FORCE



# Application of a Classical (Local) Contact Model



- Contact algorithm operates on planar facets
- Peridynamics algorithm operates on sphere elements
- Lofted geometry allows for coupling of peridynamics and contact algorithm



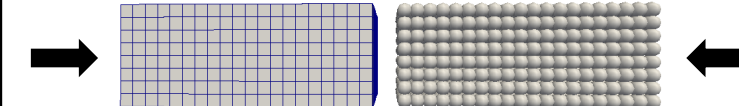
D. J. Littlewood. Simulation of dynamic fracture using peridynamics, finite element modeling, and contact. In *Proceedings of the ASME 2010 International Mechanical Engineering Congress and Exposition (IMECE)*, Vancouver, British Columbia, Canada, 2010.

SIERRA Solid Mechanics Team. Sierra/SolidMechanics 4.36 user's guide. SAND Report 2015-2199, Sandia National Laboratories, Albuquerque, NM and Livermore, CA.

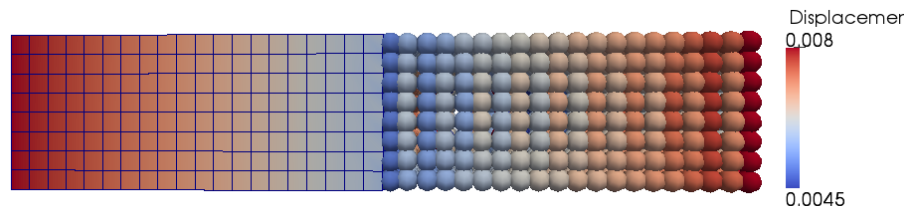
# Interface Issues with Contact Models for Peridynamics



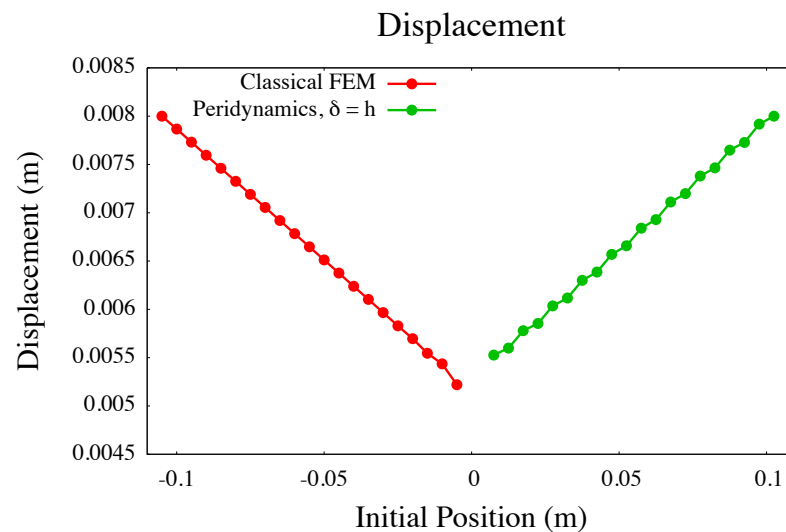
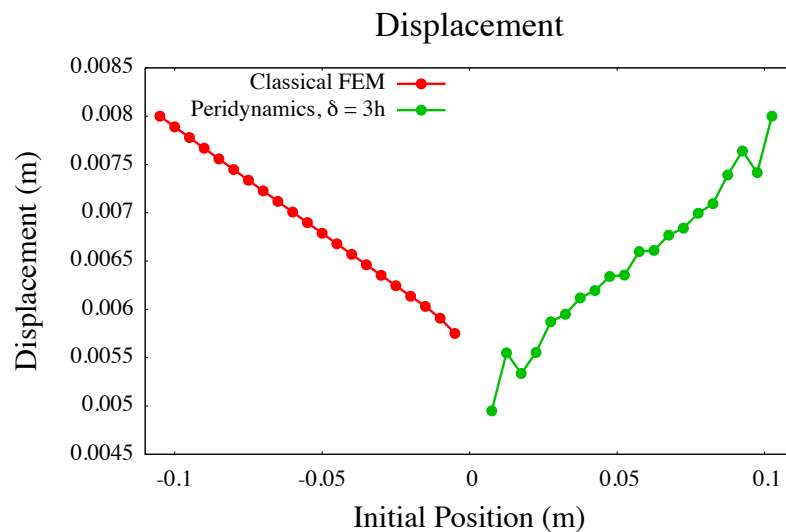
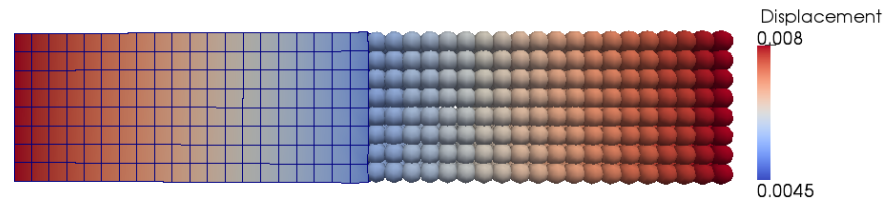
Simple Example:  
Bars Contacting in Compression



Standard Horizon  
Horizon = 3 \* Mesh Spacing



Reduce Horizon  
Horizon = Mesh Spacing



# Ingredients for Computational Peridynamics

- Constitutive model
- Bond-failure law
- Contact model
- **Discretization**
- Time integration
  - Explicit
  - Implicit
- Pre- and post-processing
- Model coupling

# Discretization Options for Peridynamic Models

## *CREATING A DISCRETIZATION FOR USE WITH PERIDIGM*

### Option 1) Genesis file

- Cubit mesh generator (hexahedron or tetrahedron mesh)
- Designate blocks and node sets
- Genesis sphere meshes also supported

### Option 2) Text file

- Discretization defined by (coordinates, volume, block id) at each node
- User-supplied node sets (lists of node ids)
- Supports EMU input files

### Option 3) Internal mesh generator

- Rectangular or cylindrical solid
- Restricted to single block
- User-supplied node sets (lists of node ids)

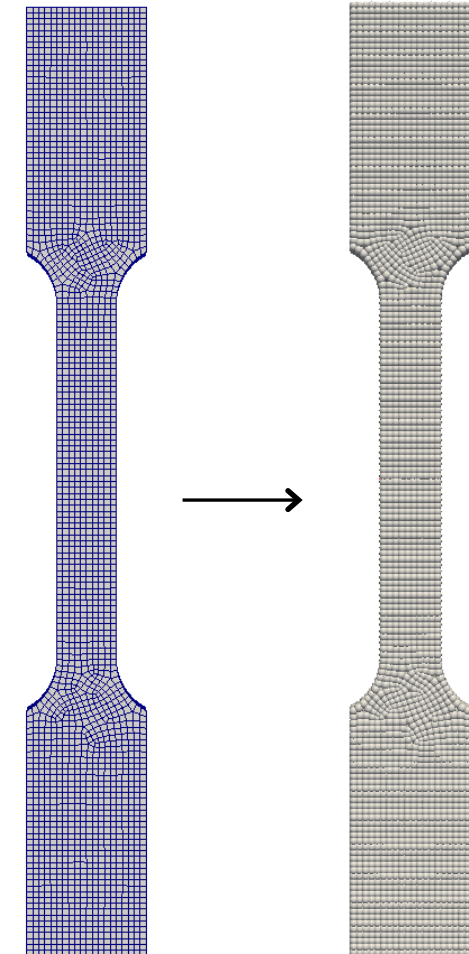
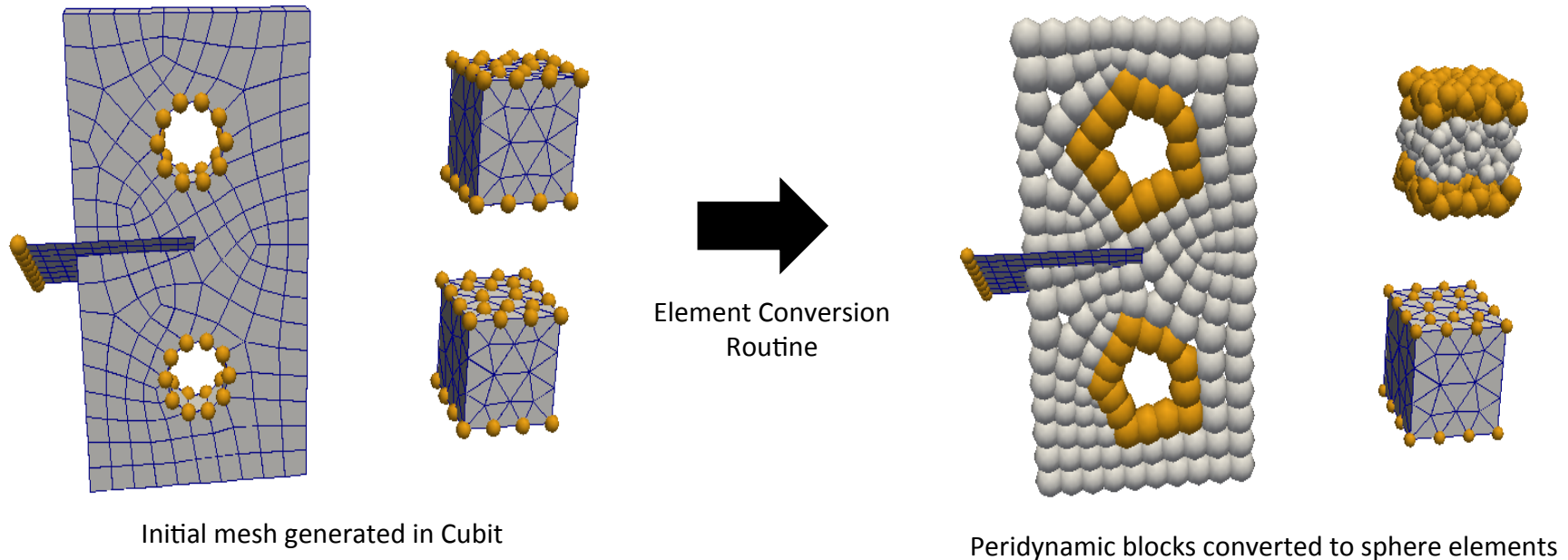


Illustration of *Peridigm* conversion  
from hexahedron mesh to sphere mesh

# Discretization Options for Peridynamic Models

## HANDLING NODE SETS AND VISIBILITY CRITERIA

- Node sets defined in the original hex/tet mesh must be transferred to meshless discretization
- Mechanism required for treating small features, controlling visibility between material points



# Convergence of Meshfree Peridynamic Simulations

## *MESHFREE APPROACH OF SILLING AND ASKARI IS WIDELY USED*

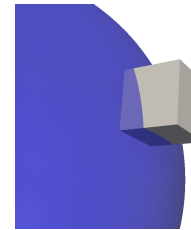
- Provides natural mechanism for material separation
- Computationally efficient, resilient

## *BUT... CONVERGENCE IS DIFFICULT TO DEMONSTRATE*

- Two forms of convergence: horizon and mesh spacing
- Current practice introduces errors and spoils convergence

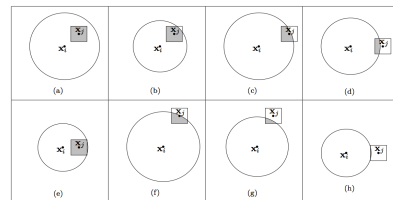
### Key Issue

Calculate horizon-element intersections

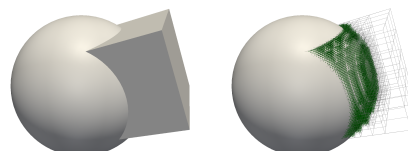


### Partial area / volume calculations

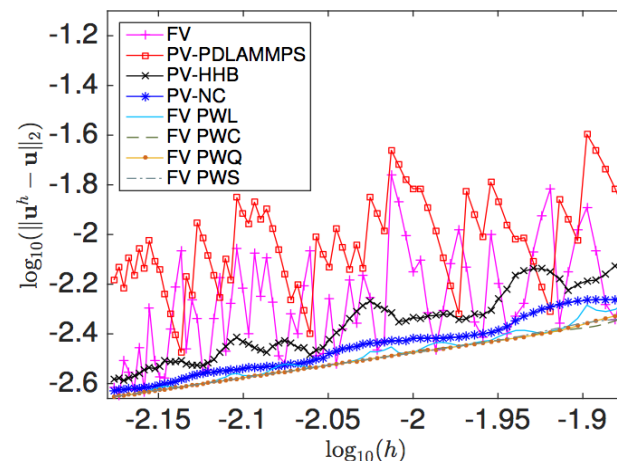
Analytical approach in 2D



Numerical approach in 3D



Modified approaches show dramatically improved convergence behavior



Seleson, P. Improved one-point quadrature algorithms for two-dimensional peridynamic models based on analytical calculations, *CMAME*, 282, pp. 184-217, 2014.

Seleson, P., and Littlewood, D. Convergence studies in meshfree peridynamic simulations. *Computers and Mathematics with Applications*. To appear.

# Ingredients for Computational Peridynamics

- Constitutive model
- Bond-failure law
- Contact model
- Discretization
- Time integration
  - Explicit
  - Implicit
- Pre- and post-processing
- Model coupling

# Time Integration

## INTEGRATION SCHEMES

- Explicit dynamics: Velocity-Verlet (leapfrog) time integrator
- Implicit dynamics: Newmark-beta
- Quasi-statics
  - Newton and Newton-like nonlinear solvers
  - Jacobian-Free Newton Krylov

## LINEAR SOLVERS

- Iterative Krylov methods, parallel scalability
- Conjugate gradient solver (default solver)

## CONSTRUCTION OF THE TANGENT MATRIX

- Construction of the tangent matrix
  - User-supplied tangent
  - Finite-difference scheme
  - *Automatic differentiation* via the *Trilinos Sacado* package
- Finite-difference scheme operates directly on internal-force calculation
  - No additional development required by material model developer
- Automatic differentiation approach requires C++ templates and (minor) extension of material model

# Explicit Time Integration

- Appropriate for dynamic problems and those with pervasive material failure
- Conditionally stable
- Requires estimate of the critical time step
- Requires many small time steps

---

## Algorithm 1 Velocity Verlet

---

$$1: \mathbf{v}^{n+1/2} = \mathbf{v}^n + \frac{\Delta t}{2} \mathbf{M}^{-1} (\mathbf{f}^n + \mathbf{b}^n)$$

$$2: \mathbf{u}^{n+1} = \mathbf{u}^n + \Delta t \mathbf{v}^{n+1/2}$$

$$3: \mathbf{v}^{n+1} = \mathbf{v}^{n+1/2} + \frac{\Delta t}{2} \mathbf{M}^{-1} (\mathbf{f}^{n+1} + \mathbf{b}^{n+1})$$

---

# Estimating the Critical Time Step

## CANDIDATE APPROACHES

- Courant-Friedrichs-Lowy (CFL) condition <sup>1</sup>
- Approach of Silling and Askari for microelastic materials (von Neumann analysis) <sup>2</sup>
- Generalized Silling and Askari approach incorporating bond angles
- Global estimate using the Lanczos method <sup>1,3</sup>
- Largest eigenvalue of 3x3 nodal stiffness matrix

## MEASURES OF SUCCESS

- Accuracy of estimate
- Computational expense

## STRATEGY FOR ASSESSING CRITICAL TIME STEP ESTIMATES

- Evaluate via test simulations
- Compare against empirical result
  - Stable time step determined by numerical experiment

1. Hughes, T.J.R. *The Finite Element Method: Linear Static and Dynamic Finite Element Analysis*. Prentice-Hall, Inc., Englewood Cliffs, NJ, 1987.
2. Silling, S.A. and Askari, E. A meshfree method based on the peridynamic model of solid mechanics. *Computers and Structures* 83:1526-1535, 2005.
3. Koteras, J.R. and Lehoucq, R.B. Estimating the critical time-step in explicit dynamics using the Lanczos method. *International Journal for Numerical Methods in Engineering* 69:2780-2788, 2007.

# Estimating the Critical Time Step

## APPROACH OF SILLING AND ASKARI FOR PROTOTYPE MICROELASTIC BRITTLE MATERIAL

$$\Delta t_c = \sqrt{\frac{2\rho}{\sum_p V_p C_{ip}}} \quad C_{ip} = |\mathbf{C}(x_p - x_i)| = \left| \frac{\partial \mathbf{f}}{\partial \boldsymbol{\eta}} \right|$$

- Derived for one-dimensional problems with bond-based PMB material model
- Anecdotal evidence suggests time step estimate is conservative for other materials

## CFL LIMIT

$$c = \sqrt{\frac{k}{\rho}} \quad \Delta t \leq \frac{\Delta x}{c}$$

- What is the proper characteristic length for peridynamic models?
- Anecdotal evidence suggests node spacing yields conservative estimate, horizon yields non-conservative estimate

## EIGENVALUE ANALYSIS

$$\mathbf{M}\ddot{\mathbf{u}} + \mathbf{K}\mathbf{u} = \mathbf{f} \quad (\mathbf{K} - \lambda\mathbf{M})\mathbf{x} = 0 \quad \Delta t_c = \frac{2}{\sqrt{\lambda}}$$

- Requires an efficient algorithm to find the maximum global eigenvalue
  - E.g., Lanczos algorithm

# Test Case: Elastic Wave Propagation

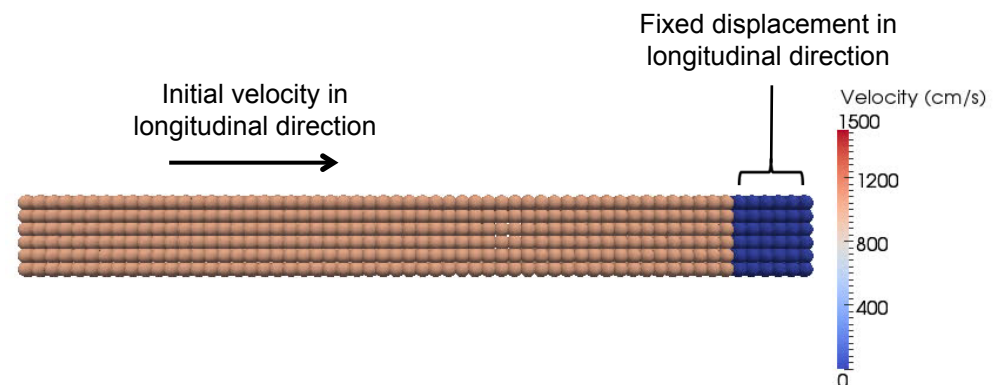
- Investigate material models
  - Microelastic bond-based
  - Linear peridynamic solid state-based
  - Wrapped classical elastic model
- Investigate critical time step estimates
  - Empirical (numerical experiment)
  - 1D approach of Silling and Askari
  - Generalized Silling and Askari
  - Element time step (3x3 stiffness probe)
  - Lanczos global estimate

Material Parameters

Density	7.8 g/cm <sup>3</sup>
Young's Modulus	300.0 GPa
Poisson's Ratio	0.25
Horizon	0.5075 cm

Simulation

Bar Length	10.0 cm
Bar Width	1.0 cm
Initial Velocity	10.0 m/s
Time Step	0.48 $\mu$ s



# Linear Peridynamic Solid State-Based Material Model

Time Step	Kinetic Energy
0.1 $\mu$ s	3.51 J
0.2 $\mu$ s	3.51 J
0.3 $\mu$ s	3.51 J
0.4 $\mu$ s	NaN
0.5 $\mu$ s	NaN
0.6 $\mu$ s	NaN
0.7 $\mu$ s	NaN
0.8 $\mu$ s	NaN
0.9 $\mu$ s	NaN
1.0 $\mu$ s	NaN

## Nodal Stiffness Matrix

max. time step = 0.314  $\mu$ s  
max. kinetic energy = 3.51 J

## CFL Limit (element size)

max. time step = 0.329  $\mu$ s  
max. kinetic energy = 3.51 J

## Empirical Observation

max. time step = 0.381  $\mu$ s  
max. kinetic energy = 3.51 J

## Global Lanczos

max. time step = 0.381  $\mu$ s  
max. kinetic energy = 3.51 J

## CFL Limit (horizon)

max. time step = 1.00  $\mu$ s  
max. kinetic energy = **unstable**

# Test Case: Fragmenting Ring

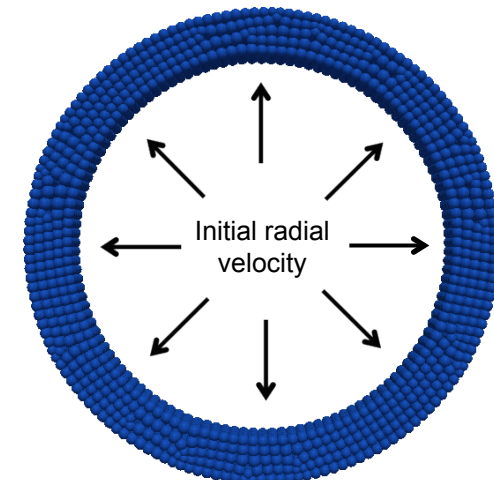
- Investigate material models
  - Microelastic bond-based
  - Linear peridynamic solid state-based
  - Wrapped classical elastic model (nosb)
- Investigate critical time step estimates
  - Empirical
  - 1D approach of Silling and Askari
  - Generalized Silling and Askari
  - Element time step (3x3 stiffness probe)
  - Lanczos global estimate

Material Parameters

Density	7.8 g/cm <sup>3</sup>
Young's Modulus	300.0 GPa
Poisson's Ratio	0.25
Critical Stretch	0.01 cm/cm
Horizon	0.603 cm

Simulation

Ring Diameter	4.5 cm
Ring Width	1 cm
Initial Radial Velocity	200.0 m/s

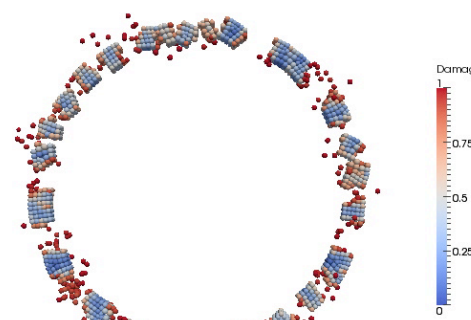


# Unstable Time Step Manifests as Increased Bond Failure

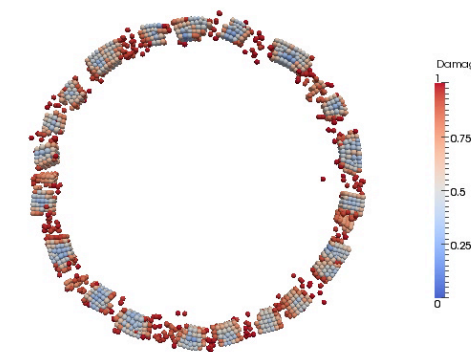


## Simulation results for microelastic material

Time Step	Percentage of Broken Bonds	Maximum Kinetic Energy ( $t > 10 \mu\text{s}$ )
$0.01 \mu\text{s}$	44.3 %	3.83 kJ
$0.1 \mu\text{s}$	44.5 %	3.82 kJ
$0.2 \mu\text{s}$	44.7 %	3.82 kJ
$0.3 \mu\text{s}$	45.3 %	3.82 kJ
$0.4 \mu\text{s}$	45.3 %	3.82 kJ
$0.5 \mu\text{s}$	45.4 %	3.82 kJ
$0.6 \mu\text{s}$	46.7 %	3.81 kJ
$0.7 \mu\text{s}$	49.1 %	3.83 kJ
$0.8 \mu\text{s}$	73.5 %	3.82 kJ
$0.9 \mu\text{s}$	95.3 %	4.39 kJ
$1.0 \mu\text{s}$	99.1 %	6.40 kJ



Time step =  $5.0 \mu\text{s}$   
46.7% of bonds broken



Time step =  $7.5 \mu\text{s}$   
62.7 % of bonds broken

# Linear Peridynamic Solid State-Based Material Model

Time Step	Percentage of Broken Bonds	Maximum Kinetic Energy ( $t > 10 \mu\text{s}$ )
0.01 $\mu\text{s}$	40.3 %	3.43 kJ
0.1 $\mu\text{s}$	40.2 %	3.43 kJ
0.2 $\mu\text{s}$	40.4 %	3.43 kJ
0.3 $\mu\text{s}$	41.6 %	3.42 kJ
0.4 $\mu\text{s}$	42.0 %	3.44 kJ
0.5 $\mu\text{s}$	44.7 %	3.45 kJ
0.6 $\mu\text{s}$	95.6 %	4.33 kJ
0.7 $\mu\text{s}$	97.3 %	5.54 kJ
0.8 $\mu\text{s}$	98.6 %	7.14 kJ
0.9 $\mu\text{s}$	99.4 %	19.8 kJ
1.0 $\mu\text{s}$	99.8 %	62.8 kJ

## CFL Limit (element size)

max. time step = 0.395  $\mu\text{s}$   
percentage of broken bonds = 45.3 %  
max. kinetic energy = 3.51 J

## Global Lanczos

max. time step = 0.494  $\mu\text{s}$   
percentage of broken bonds = 42.8 %  
max. kinetic energy = 3.43 kJ

## Nodal Stiffness Matrix

max. time step = 0.505  $\mu\text{s}$   
percentage of broken bonds = 44.8 %  
max. kinetic energy = 3.82 kJ

## Empirical Observation

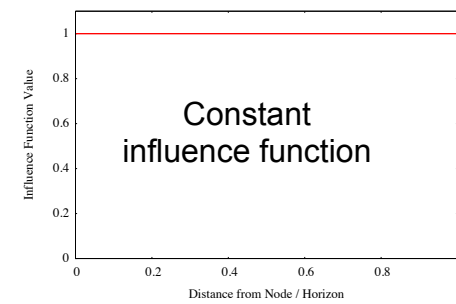
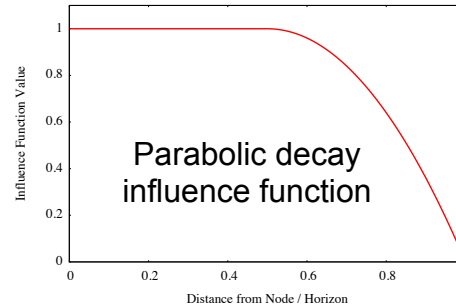
max. time step = 0.509  $\mu\text{s}$   
percentage of broken bonds = 50.0 %  
max. kinetic energy = 3.46 kJ

## CFL Limit (horizon)

max. time step = 1.19  $\mu\text{s}$   
percentage of broken bonds = 99.1 %  
max. kinetic energy = **unstable**

# The Influence Function Affects the Critical Time Step

- Choice of influence function affects critical time step
- Lanczos algorithm successfully detects changes in critical time step
- Observation: Influence function that decays with increasing bond length results in reduced critical time step



Peridynamic Linear Solid

	Parabolic decay influence function	Constant influence function
Max. Lanczos time step	0.381 $\mu$ s	0.434 $\mu$ s
Empirical result	0.381 $\mu$ s	0.434 $\mu$ s

14% Increase

Wrapped Classical Material Model

	Parabolic decay influence function	Constant influence function
Max. Lanczos time step	0.490 $\mu$ s	0.549 $\mu$ s
Empirical result	0.490 $\mu$ s	0.549 $\mu$ s

12% Increase

# Implicit Time Integration

- Unconditionally stable
- Allows for large time steps
- Allows for solution of static and quasi-static problems
  - Neglect dynamic effects
- Requires solution of system of equations involving current and future configurations
  - Generally nonlinear
  - Newton-like methods require tangent stiffness matrix
  - Matrix-free approaches offer alternative approach

# Construction of the Tangent Stiffness Matrix

---

**Algorithm 1** Construction of the tangent stiffness matrix by central finite difference.

---

```

1: procedure TANGENT STIFFNESS MATRIX
2:    $\triangleright$  Initialize the tangent stiffness matrix to zero.
3:    $\mathbf{K} \leftarrow \mathbf{0}$ 
4:    $\triangleright$  Traverse each node in the discretization.
5:   for each node  $i$  do
6:      $\{traversal\ list\} \leftarrow$  node  $i$  and all neighbors of node  $i$ 
7:     for each node  $j$  in  $\{traversal\ list\}$  do
8:        $\triangleright$  Evaluate the force state at  $\mathbf{x}_i$  under perturbations of displacement.
9:       for each displacement degree of freedom  $r$  at node  $j$  do
10:       $\underline{\mathbf{T}}^{\epsilon+} \leftarrow \underline{\mathbf{T}}[\mathbf{x}_i](\mathbf{u} + \epsilon^r)$ 
11:       $\underline{\mathbf{T}}^{\epsilon-} \leftarrow \underline{\mathbf{T}}[\mathbf{x}_i](\mathbf{u} - \epsilon^r)$ 
12:       $\triangleright$  Evaluate pairwise forces under perturbations of displacement.
13:      for each node  $k$  in neighbor list of node  $i$  do
14:         $\mathbf{f}^{\epsilon+} \leftarrow \underline{\mathbf{T}}^{\epsilon+} \langle \mathbf{x}_k - \mathbf{x}_i \rangle \Delta V_i \Delta V_k$ 
15:         $\mathbf{f}^{\epsilon-} \leftarrow \underline{\mathbf{T}}^{\epsilon-} \langle \mathbf{x}_k - \mathbf{x}_i \rangle \Delta V_i \Delta V_k$ 
16:         $\mathbf{f}^{\text{diff}} \leftarrow \mathbf{f}^{\epsilon+} - \mathbf{f}^{\epsilon-}$ 
17:        for each degree of freedom  $s$  at node  $k$  do
18:           $K_{sr} \leftarrow K_{sr} + \frac{f_s^{\text{diff}}}{2\epsilon}$ 
19:        end for
20:      end for
21:    end for
22:  end for
23: end for
24: end procedure

```

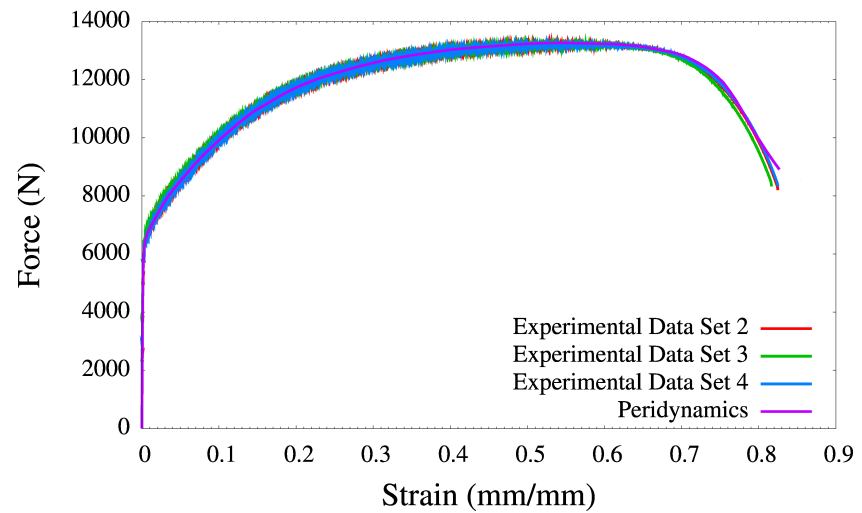
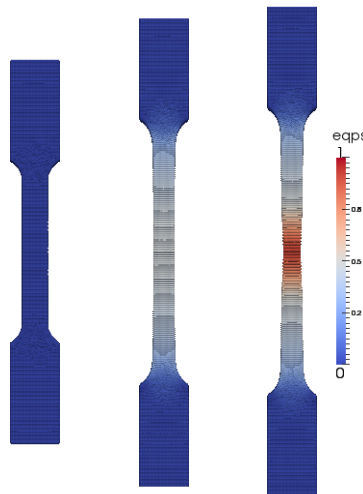
---

# Dogbone Tensile Test

## CONSTITUTIVE MODEL CALIBRATION AGAINST EXPERIMENTAL DATA

- Dogbone specimen
  - 304L stainless steel (very ductile)
  - Quasi-static loading conditions
- Peridynamic model
  - Non-ordinary state-based peridynamic
  - Elastic-plastic material constitutive model with piece-wise hardening curve

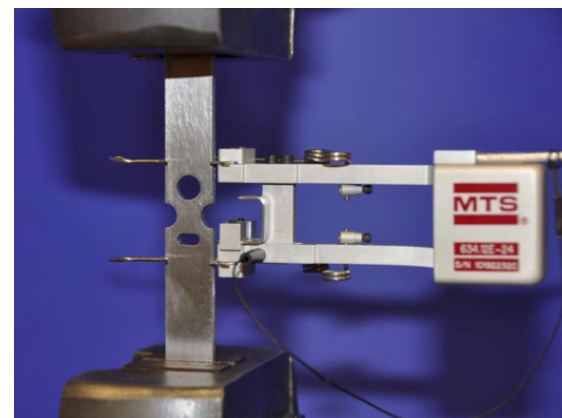
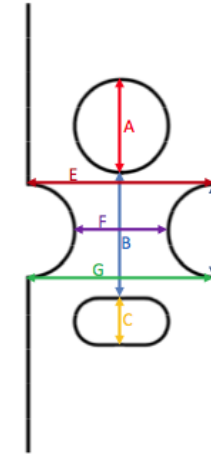
Young's Modulus	200.0 GPa
Poisson's Ratio	0.285
Yield Stress	220.0 MPa



# Necking Experiment

*CAN A PERIDYNAMIC MODEL CAPTURE LOCALIZATION?*

- Specimen
  - 304L stainless steel (very ductile)
  - Quasi-static loading conditions
- Quantities of interest
  - Record force and engineering strain at peak load
  - Record engineering strain when force has dropped to 95% of peak load
  - Record chord lengths when force has dropped to 95% of peak load

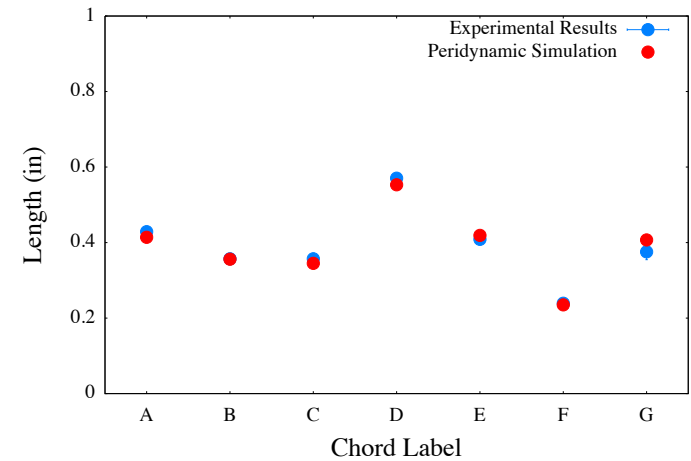
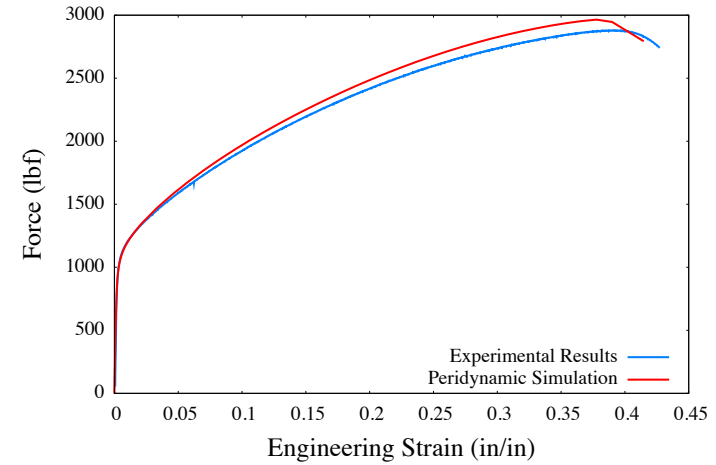
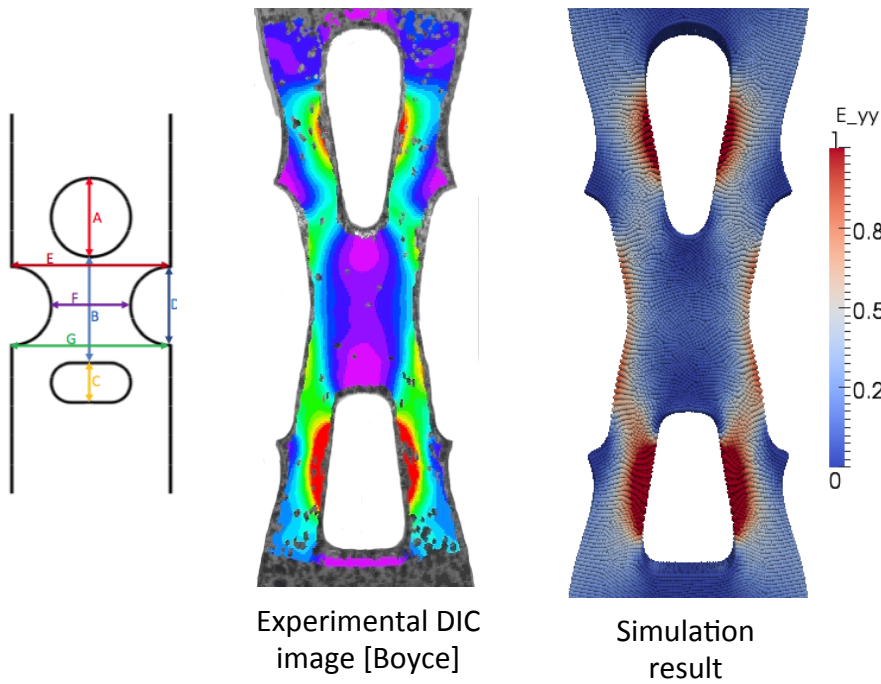


Experimental setup [Boyce]

# Necking Experiment

## PERIDYNAMIC MODEL

- Refined discretization contained 2,104,860 elements
- Peridynamic horizon approximately 1/10<sup>th</sup> the size of smallest geometric features



# Modal Analysis of a Simply-Supported Beam

## BENCHMARK PROBLEM FOR MODAL ANALYSIS

- One-dimensional analysis of simply-supported beam with square cross section

## KEY ISSUES

- Does the peridynamic model agree with the classical (local) analytic solution in the case of a small horizon?
- How does solution of the peridynamic (nonlocal) model compare with a classical finite element solution of the local model?

### Classical (local) analytic solution

$E$	Elastic modulus
$h$	Height and depth of beam
$m$	Mass of beam
$l$	Length of beam
$n$	Positive integer
$f_n$	Characteristic linear frequency (mode $n$ )

$$f_n = \frac{n^2 \pi}{2} \sqrt{\frac{E h^4}{12 m l^4}}$$

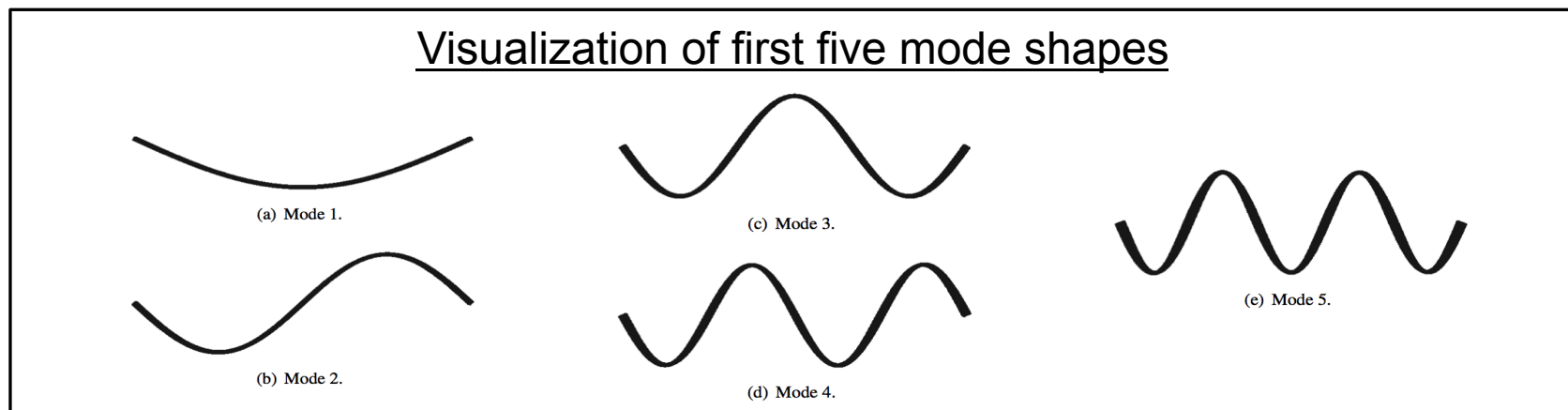


# Modal Analysis of a Simply-Supported Beam

## *PERIDYNAMIC SIMULATION*

- Beam dimensions: 1m x 0.01m x 0.01m
- Material: steel ( $E = 206.8$  GPa)
- Peridynamic horizon: 0.000713m
- Classical linear elastic material model applied via non-ordinary state-based peridynamics
- Emulation of one-dimensional problem
- Discretized with 840K elements

Mode	Classical Theory	Peridynamic Simulation	Percent Difference
1	23.30 Hz	23.26 Hz	0.17 %
2	93.22 Hz	93.02 Hz	0.21 %
3	209.73 Hz	209.06 Hz	0.32 %
4	372.86 Hz	371.29 Hz	0.43 %
5	582.59 Hz	579.39 Hz	0.55 %



David J. Littlewood, Kyran Mish, and Kendall Pierson. 2012. Peridynamic simulation of damage evolution for structural health monitoring. Proceedings of the ASME 2012 International Mechanical Engineering Congress and Exposition (IMECE2012), Houston, TX.

# Jacobian-Free Newton Krylov



## *MATRIX-FREE APPROACH SHOWS PROMISE FOR PERIDYNAMIC MODELS*

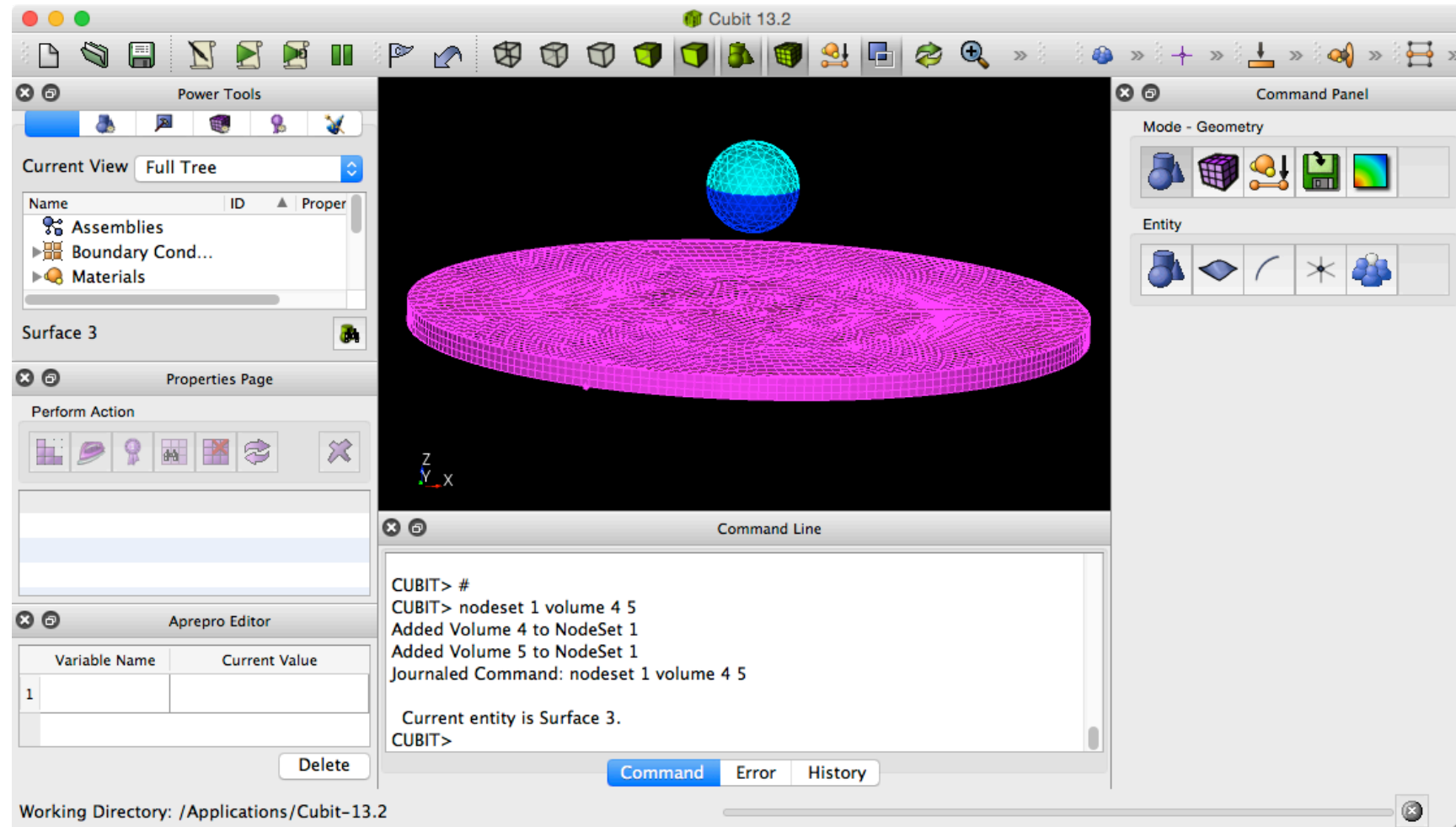
- Allows for solution of linear system without explicit construction of tangent stiffness matrix
- Attractive for peridynamics due to high computational cost of assembling and solving matrix-vector system
- Initial results show dramatic reduction in computational expense and memory usage

# Ingredients for Computational Peridynamics

- Constitutive model
- Bond-failure law
- Contact model
- Discretization
- Time integration
  - Explicit
  - Implicit
- Pre- and post-processing
- Model coupling

# Performing a Peridynamic Simulation

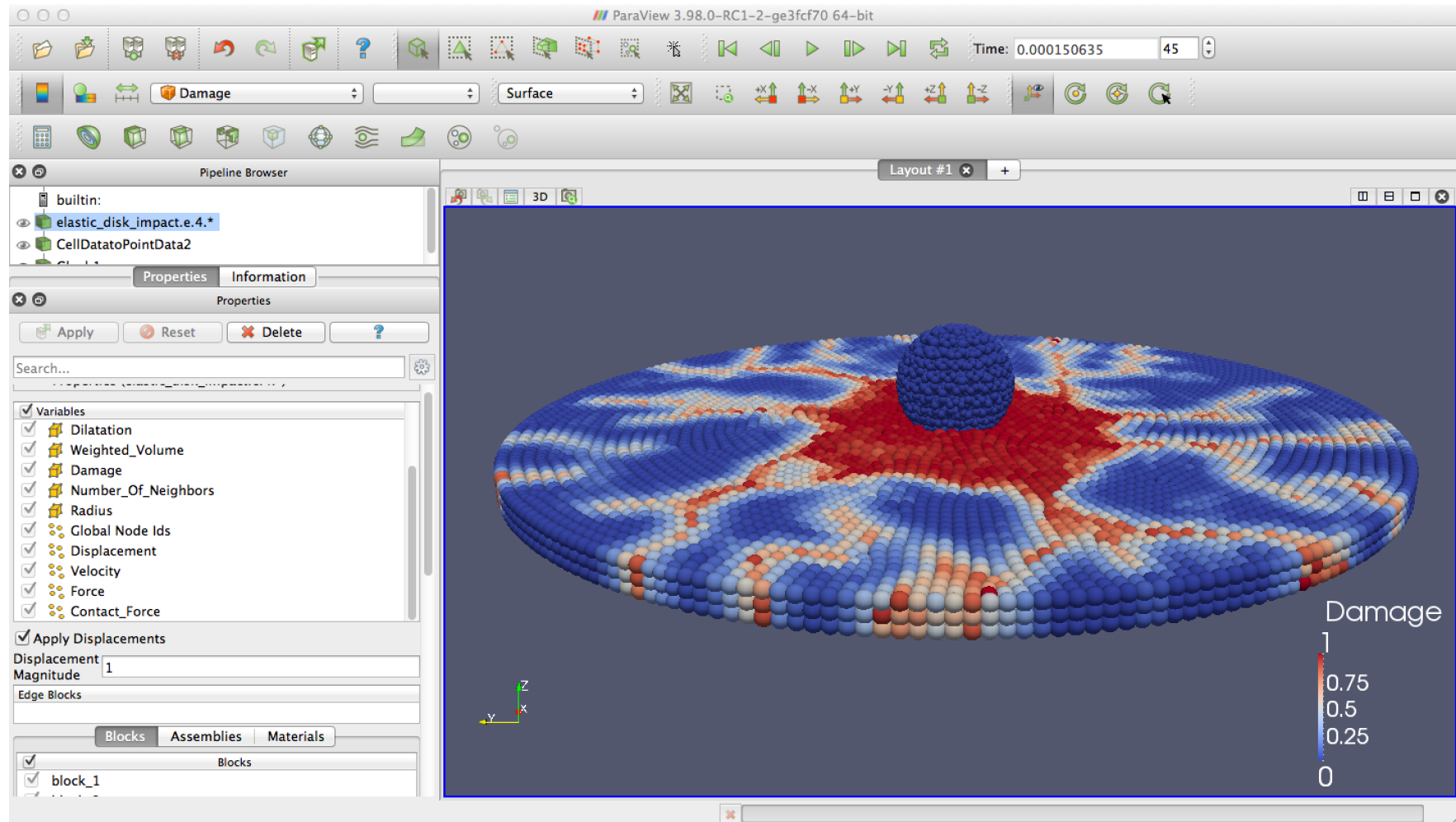
## PRE-PROCESSING WITH CUBIT<sup>1</sup>



1. cubit.sandia.gov

# Performing an Peridynamic Analysis

## POST-PROCESSING WITH PARAVIEW<sup>1</sup>



1. [www.paraview.org](http://www.paraview.org)

# Ingredients for Computational Peridynamics

- Constitutive model
- Bond-failure law
- Contact model
- Discretization
- Time integration
  - Explicit
  - Implicit
- Pre- and post-processing
- **Model coupling**

# A Variable Peridynamic Horizon is Required to Achieve Compatibility at Local-Nonlocal Interfaces

## PERIDYNAMIC PARTIAL STRESS FORMULATION

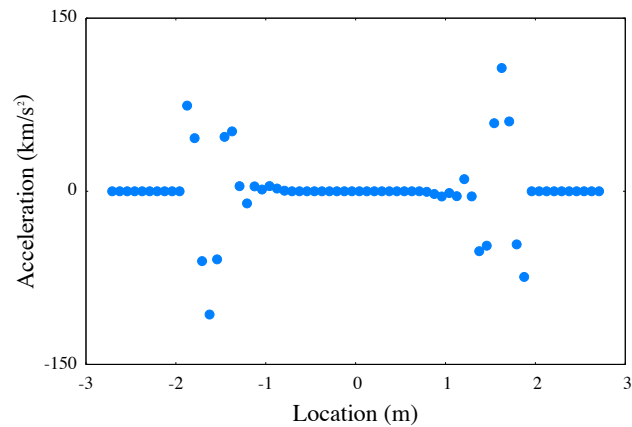
- Standard peridynamic models do not allow for a variable nonlocal length scale
- Peridynamic partial stress was developed specifically to support a variable horizon

$$\nu_o(\mathbf{x}) := \int_{\mathcal{H}} \mathbf{T}[\mathbf{x}] \langle \xi \rangle \otimes \xi \, dV_{\mathbf{x}'}$$

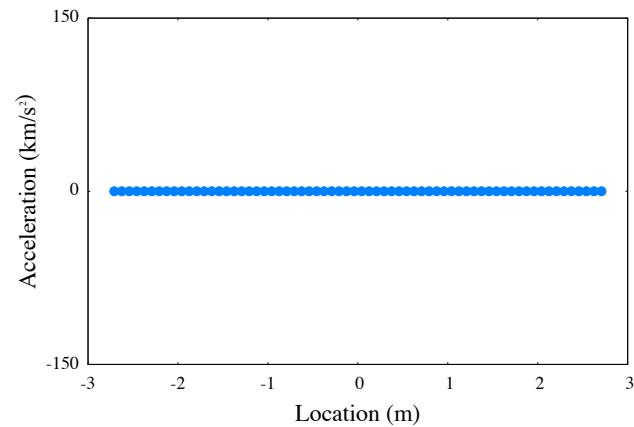
- Partial stress formulation is guaranteed to pass the linear patch test, performs well under smooth deformation (as in coupling region)

### Test case

Prescribed linear displacement over a bar with a varying peridynamic horizon



Varying the horizon disrupts the standard model

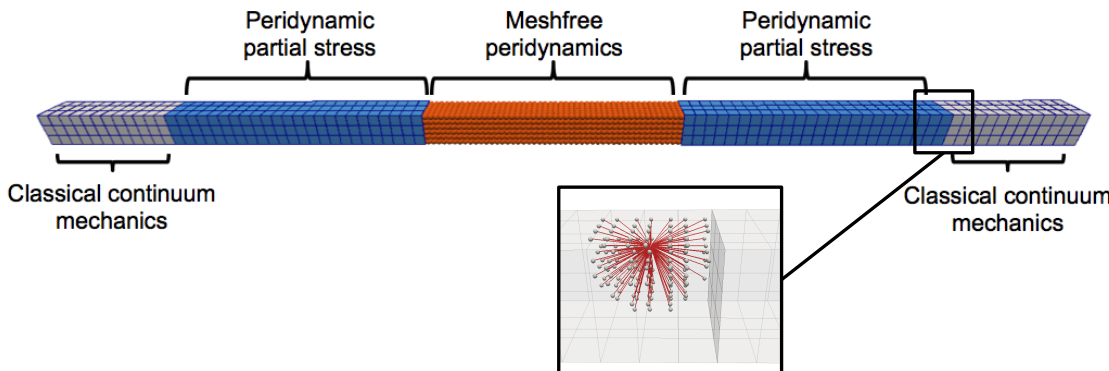


Partial stress formulation dramatically improves results

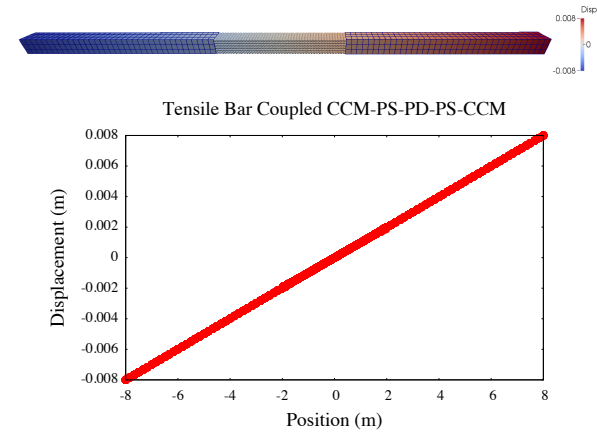
# The Partial Stress Formulation for Local-Nonlocal Coupling



- Software infrastructure in place for strongly coupled simulations
- Meshfree peridynamic models, peridynamic partial stress, and classical FEM within single executable
- Partial stress provides transition between classical continuum mechanics and peridynamics
- Monolithic implicit solve (statics)
- Local-nonlocal coupling allows for application of local-only BC



Patch test results



# Leveraging the LDRD: Optimization-Based Coupling

## ONGOING EFFORT OF D'ELIA, PEREGO, AND BOCHEV

- Model coupling can be cast as an optimization problem
  - *Objective function*: Difference between solutions in overlap region
  - *Constraints*: Governing equations of the individual models
  - *Controls*: Fictitious boundary conditions in overlap region

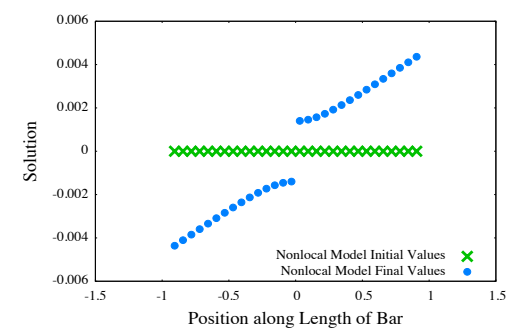
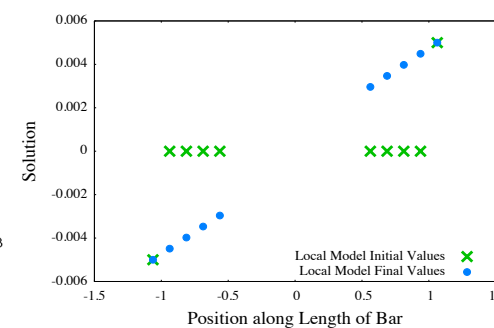
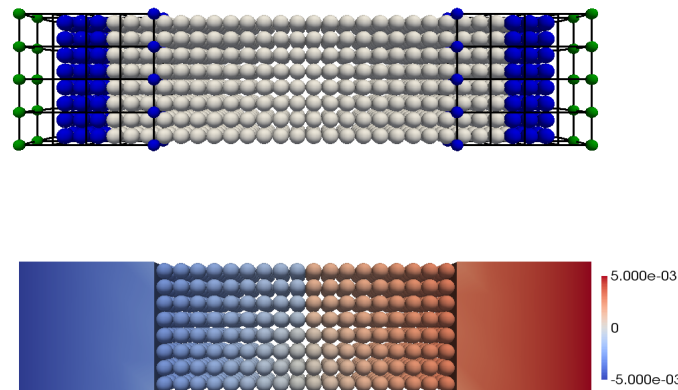
Peridigm

Albany

Trilinos

## COLLABORATIVE EFFORT FOR ALBANY-PERIDIGM COUPLING

- Leverages LDRD and agile components approach
- Demonstration simulations couple local and nonlocal diffusion models



D'Elia, M., Perego, M., Bochev, P., Littlewood, D. A coupling strategy for nonlocal and local diffusion models with mixed volume constraints and boundary conditions. *Computers and Mathematics with Applications*. Submitted for publication.

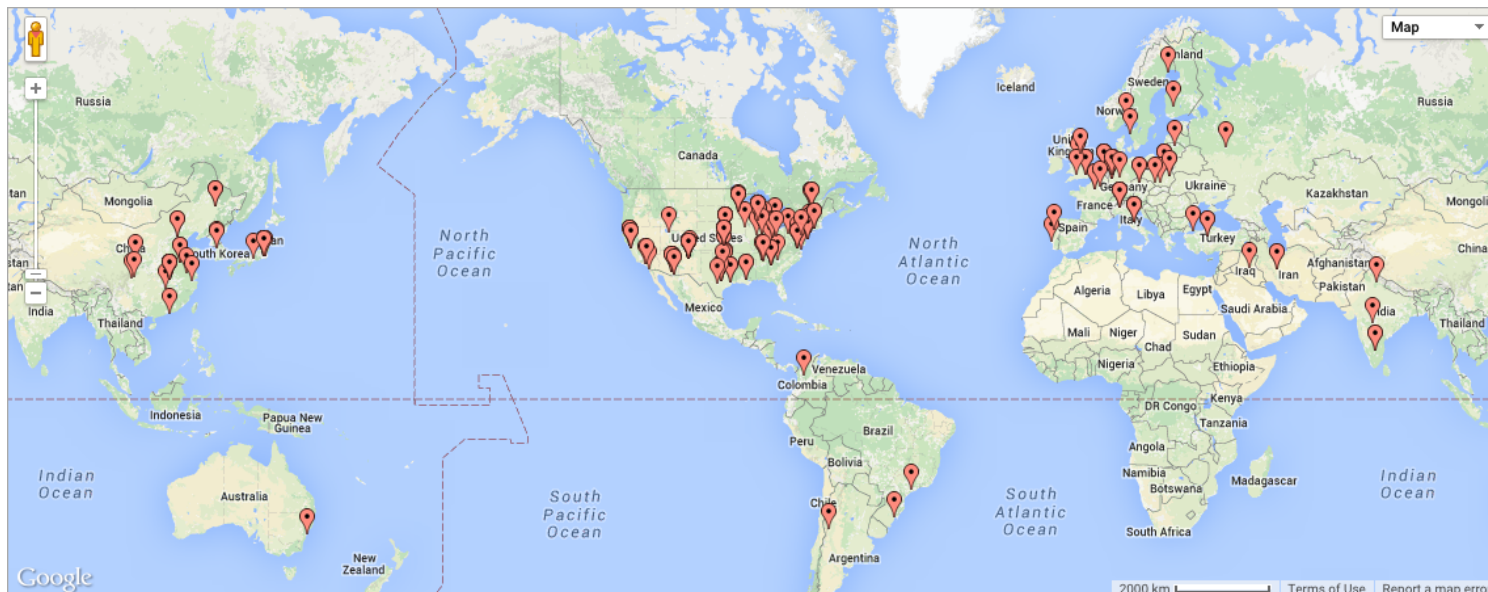
# Questions?

David Littlewood

[djlitt@sandia.gov](mailto:djlitt@sandia.gov)

<http://peridigm.sandia.gov>

*Peridigm Downloads (July 2014 – August 2015)*



Map generated at <http://batchgeo.com>